Biometals
DOI 10.1007/s10534-010-9390-5

Conformational study of bovine lactoferricin in membrane-micking conditions by molecular dynamics simulation and circular dichroism

Isabella Daidone · Alessandro Magliano · Alfredo Di Nola · Giuseppina Mignogna · Matilda Manuela Clarkson · Anna Rita Lizzi · Arduino Oratore · Fernando Mazza

Received: 26 July 2010 / Accepted: 7 November 2010

Abstract Lactoferricins are potent antimicrobial peptides released by pepsin cleavage of Lactoferrins. Bovine Lactoferricin (LfcinB) has higher activity than the intact bovine Lactoferrin, and is the most active among the other Lactoferricins of human, murine and caprine origin. In the intact protein the fragment corresponding to LfcinB is in an helical conformation, while in water LfcinB adopts an amphipathic β-hairpin structure. However, whether any of these structural motifs is the antibacterial active conformation, i.e., the one interacting with bacterial membrane components, remains to be seen. Here we present Circular Dichroism (CD) spectra and Molecular Dynamics (MD) simulations indicating that in membrane-mimicking solvents the LfcinB adopts an amphipathic β-hairpin structure similar to that observed in water, but differing in the dynamic behavior of the side-chains of the two tryptophan residues. In the membrane-mimicking solvent these side-chains show a high propensity to point towards the hydrophobic environment, rather than being in the hydrophobic core as seen in water, while the backbone preserves the hairpin conformation as found in water. These results suggest that the tryptophans might act as anchors pulling the stable, solvent-invariant hairpin structure into the membrane.

Keywords Antimicrobial peptides · Molecular dynamics simulation · Circular dichroism · Amphipathic · β-hairpin

Oratore Arduino—Deceased.

I. Daidone
Department of Chemistry, Chemical Engineering and Materials, University of L'Aquila, via Vetoio (Coppito 1), 67010 Coppito, AQ, Italy

A. Magliano · A. Di Nola
Department of Chemistry, University of Rome ''La Sapienza'', P.le Aldo Moro 5, 00185 Rome, Italy

G. Mignogna
Department of Biochemical Sciences ''A. Rossi Fanelli'', University of Rome ''La Sapienza'', P.le Aldo Moro 5, 00185 Rome, Italy

M. M. Clarkson · A. R. Lizzi · A. Oratore
Department of Biomedical Sciences and Technologies, University of L'Aquila, via Vetoio (Coppito 1), 67010 Coppito, AQ, Italy

F. Mazza (✉)
Department of Health Sciences, University of L'Aquila, via Vetoio (Coppito 1), 67010 Coppito, AQ, Italy
e-mail: fernando.mazza@univaq.it

Introduction

Antimicrobial peptides represent good candidates for the development of new antibiotic drugs due to their broad antimicrobial spectra, rapid killing and rare development of drug resistance (Boman 1995; Ganz and Lehrer 1999; Hancock 2001; Zasloff 2002). Peptides with antimicrobial activity show a wide

Published online: 19 November 2010

variety of structural motifs which encompasses α-helices, antiparallel β-sheets and relaxed coils. Despite the extremely high structural variability, most of the antimicrobial peptides share many chemico-physical and biological properties: they are charged at physiological pH, amphiphilic, active against bacteria, fungi, viruses and protozoa (Martin et al. 1995) and often originate from precursor proteins through proteolytic digestion (Tomita et al. 1991; Bals and Wilson 2003).

The antimicrobial peptides Lactoferricins are released by pepsin cleavage of Lactoferrins, iron-binding glycoproteins present in milk. It was reported that bovine Lactoferricin (LfcinB) has antimicrobial activity higher than the intact protein bovine Lactoferrin (LfB) (Bellamy et al. 1992a, b; Bellamy et al. 1994), and that it is the most active among the other Lfcins of human, murine and caprine origin (Vorland et al. 1998). Moreover, not only is LfcinB active against gram-positive as well as gram-negative bacteria, fungi, and protozoa (Bellamy et al. 1994; Gifford et al. 2005), but it also shows antiviral and antitumor properties (Anderson et al. 2003; Eliassen et al. 2002; Roy et al. 2002).

LfcinB is a 25 amino acid peptide released from the N-terminal part of LfB, with the sequence ^{17}FKCRRWQWRMKKLGAPSITCVRRAF^{41}. The two C residues form a disulfide bridge that is present also in LfB, though it was shown that it is not essential for the antimicrobial activity (Bellamy et al. 1992a, b). Studies of LfcinB analogs have evidenced that the two tryptophan residues, W6 and W8, as well as the cationic arginine (R) residues are essential for the antimicrobial activity (Boman 1995; Ganz and Lehrer 1999; Hancock 2001; Zasloff 2002; Strøm et al. 2000; Strøm et al. 2002; Vogel et al. 2002). In particular, the N-terminal part of LfcinB, containing the sequence RRWQWR, is the most active portion of LfcinB (Rekdal et al. 1999; Tomita et al. 1994). In fact, it was shown that a fragment composed of the first fifteen residues (F1-A15) has comparable antibacterial activity with respect to LfcinB (Rekdal et al. 1999), and even the short six-residue peptide RRWQWR corresponding to the residues 4–9, retains most of the antimicrobial activity (Tomita et al. 1994).

Synthetic peptides homologous to the portion F1-A15 of LfcinB, and with sequence of caprine, human, murine and porcine lactoferricins show much lower or no antibacterial activity (Strøm et al. 2000), which correlates to the number of tryptophans present. In fact, the bovine 15-residue is the only one containing two W residues, and it was shown that the antibacterial activity of the 15-residue fragments of non bovine lactoferricins is enhanced when two tryptophan residues are inserted in position 6 and 8 (Strøm et al. 2000).

In the crystal structure of the intact protein LfB (Moore et al. 1997), the sequence F17-L29 (corresponding to F1-L13 of LfcinB) adopts an α-helix and the segment S33-R39 (S17-R23 of LfcinB) is in a β-strand conformation. Furthermore, the R3-G14 peptide of LFcinB (R20-G30 of LfB) assumes an α-helix conformation in the presence of 2,2,2-trifluoroethanol (TFE) and sodium dodecyl sulfate (SDS) (Kang et al. 1996). Conversely, the 2D NMR spectra performed on the aqueous solution of LfcinB (Hwang et al. 1998) reveal that the peptide adopts an overall conformation corresponding to a distorted antiparallel β-sheet. This means that the tract of LfB, F17-F41, undergoes a conformational conversion once detached from the protein. The conformational transition of LFcinB was analyzed in aqueous solution with biased Molecular Dynamics (MD) simulations, whereas unbiased short simulations could not reveal the same conversion between the crystal and solution structure (Zhou et al. 2004).

The above mentioned data show that the conformation of the *N*-terminal sequence F1-L13 markedly differs depending on the environment. In water solution, it adopts an extended β-strand conformation while an α-helical structure is observed for the same region (F17-L29) in the crystal of LfB. However, structural information on LfcinB in membrane-like conditions is still missing (free energies of adsorption of LfcinB on a neutral membrane have been computed, but no structural information of the peptide inside the membrane were evaluated (Vivcharuk et al. 2008)). Conversely, the secondary structure of the less potent antimicrobial LfcinH has been analyzed both in aqueous solution and in a membrane mimicking mixture (Hunter et al. 2005). In aqueous solution LfcinH shows a partially-disordered helical structure with no evidence of β-sheet, while in the membrane mimicking (4:4:1 methanol–chloroform–water) mixture the helical content of LfcinH increases to an extent resembling the conformation that this region adopts in the crystal structure of the intact protein, LfH (Anderson et al. 1989).

Here, we present very long (on the μs timescale) atomistic MD simulations of LfcinB in water and the membrane mimicking mixture previously employed for LfcinH (4:4:1 methanol–chloroform–water) together with Circular Dichroism (CD) spectra in water and in SDS micellar and non micellar aqueous solutions. The results indicate that LfcinB adopts an amphipathic β-hairpin structure, independently from the environment, with a backbone conformation similar to that observed in water, but with differences in the conformational behavior of key tryptophan side-chains.

Materials and methods

Molecular dynamics simulations

MD simulations of LfcinB were performed in water and in the chloroform–methanol–water (4:4:1) membrane mimicking mixture using the GROMACS software package (Berendsen et al. 1995) and the GROMOS96 force field (van Gunsteren et al. 1996). The chloroform–methanol–water mixture was chosen because already adopted in the experiments on the LfcinH (Hunter et al. 2005). Two different structures, the β-hairpin (PDB entry 1LFC) and the α-helix adopted by the peptide fragment in the crystal structure of LfB (residues 17–41 from the PDB entry 1BLF), were taken as starting conformations for the simulation in water and mixed solvent. Water was represented with the simple point charge (SPC) model (Berendsen et al. 1987). The parameters for chloroform and methanol were taken from the GROMOS96 force field (van Gunsteren et al. 1996).

For each starting structure, one peptide molecule was solvated, with either water or mixed solvent, in a periodic rhombic dodecahedral box large enough to contain the peptide and at least 0.8 nm of solvent on all sides. For the simulations in membrane-mimicking solvent the peptide was inserted in the center of a pre-equilibrated box of the mixture. Solvent molecules overlapping with the peptide were deleted. The simulations were performed in the NTP ensemble at the experimental temperature of 298 K and at a pressure of 1 bar. The isokinetic temperature coupling (Brown and Clarke 1984) was used to keep the temperature constant and the Berendsen pressure coupling was used to keep the pressure constant (Berendsen et al. 1984). The bond lengths were fixed (Berendsen et al. 1995) and a time step of 2 fs for numerical integration was used. Periodic boundary conditions were applied to the simulation box and the long-range electrostatic interactions were treated with the Particle Mesh Ewald method (Darden et al. 1993) using a grid spacing of 0.12 nm combined with a fourth-order B-spline interpolation to compute the potential and forces in between grid points. The real space cut-off distance was set to 0.9 nm and the van der Waals cut-off distance to 1.4 nm. The N-terminal and C-terminal ends of the peptide were modeled as NH_3^+ and CO_2^-, respectively. Eight negative counter ions were added (Cl^-) to make the simulation box neutral.

Simulation lengths of the different systems were 0.25 and 0.62 μs for the β-hairpin and α-helix, respectively, in water and 1.1 and 3.0 μs for the β-hairpin and α-helix, respectively, in the mixed solvent.

Circular dichroism measurements

All the chemicals used in the present study were pure chemical grade. In particular, LfcinB was bought from the commercial GENEPEP S.A. (France), which guaranteed an HPLC purity degree higher than 97%.

Given that some common organic solvents, such as tetrahydrofuran, chloroform and dichloromethane, are not compatible with far-UV CD, we could not perform CD analysis with the same membrane-mimicking mixture (4:4:1 methanol–chloroform–water) used in MD simulations. Therefore, in addition to water, we performed CD spectra of LfcinB samples (100 μM) in non micellar (2 mM) and micellar (20 mM) SDS solutions, that can provide an hydrophobic environment (Waterhouse and Johnson 1994).

CD spectra were carried out with a Jasco J710 spectropolarimeter, equipped with a DP 520 processor, using quartz cell with an optical path length of 1 mm. All spectra were recorded at 25°C and measured in the wavelength interval from 190 to 250 nm with a 0.5 nm step resolution and a 2 nm bandwidth. The scanning rate was 10 nm/min with 0.25 s response time. The signal to noise ratio was improved by accumulating at least five scans. Data processing was carried out using the J-710 software package. To analyze the content of secondary structure elements, CONTIN, CDSSTR and K2D methods was used on DICHROWEB server

(http://www.cryst.bbk.ac.uk/cdweb/html/home.htm) (Whitmore and Wallace 2004).

Results and discussion

Circular dichroism

The CD spectra, reported in Fig. 1, show a similar qualitative behavior, indicating that the secondary structure of LfcinB is independent from the environment conditions. A similar pattern is present in 2 mM SDS and 20 mM SDS, indicating that the presence of micellar and non micellar SDS solution has only a slight effect on the peptide secondary structure content. The position of the minimum, although at a rather low wavelength compared to that usually found for peptides in pure β-sheet structures (218 nm), suggests that the peptide structure is partly based on a β-sheet conformation. The low value of the ellipticity at 205 nm together with the lack of a positive contribution in the far UV region (around 200 nm) indicate that more than one conformation is present. The content of secondary structure was analyzed utilizing the methods CONTIN, CDSSTR and K2D. The results, summarized in Table 1, indicate that the helical population is always lower than 10%, the remaining being almost equally distributed between the unstructured and β-sheet structure. A previous study (Kang et al. 1996) reported that a higher concentration of SDS (30 mM SDS micellar solution) was required to observe a higher content of helical structure.

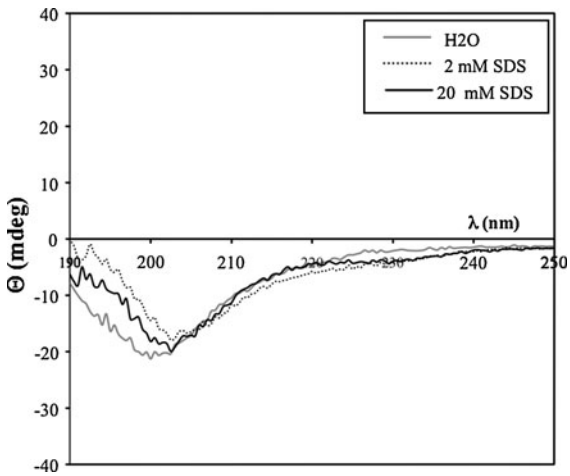

Fig. 1 The CD spectra of LfcinB (100 μM) in water, 2 mM non-micellar SDS and 20 mM micellar SDS solution at 25°C

Molecular dynamics simulations

The two simulations starting from the helical structure, one performed in water and the other in the mixed solvent, show that the helical conformation disappears after few tens of nanoseconds. Moreover, within the simulation time, the LfcinB adopts a loose hairpin-like structure (see Fig. 2). Conversely, the other two simulations starting from the hairpin structure, one performed in water and the other in the mixed solvent, show that the β-structure is maintained in both conditions throughout the full runs. In the following, we report details of the structural and dynamical properties of LfcinB along the two simulations starting from the hairpin structure.

The fluctuations of the backbone atoms of LfcinB obtained in both solvents are very similar and are reported in Fig. 3. Apart from the high fluctuations of the N- and C-terminal residues, F1-R4 and V21-F25, which are commonly observed in peptides, the highest fluctuations are observed for the residues belonging to the loop connecting the two strands, i.e., from residue M10 to A15. This agrees with the root

Table 1 Estimation of lactoferricin secondary structure motifs obtained by CONTIN, CDSSTR and K2D programs from CD data (Whitmore and Wallace 2004)

Lactoferricin (100 μM)	CONTIN			CDSSTR			K2D		
	Helix (%)	β-sheet (%)	Random (%)	Helix (%)	β-sheet (%)	Random (%)	Helix (%)	β-sheet (%)	Random (%)
H_2O	4	43	53	3	43	54	7	51	42
2 mM SDS	8	46	46	5	45	50	8	46	46
20 mM SDS	10	47	43	6	46	48	7	49	43

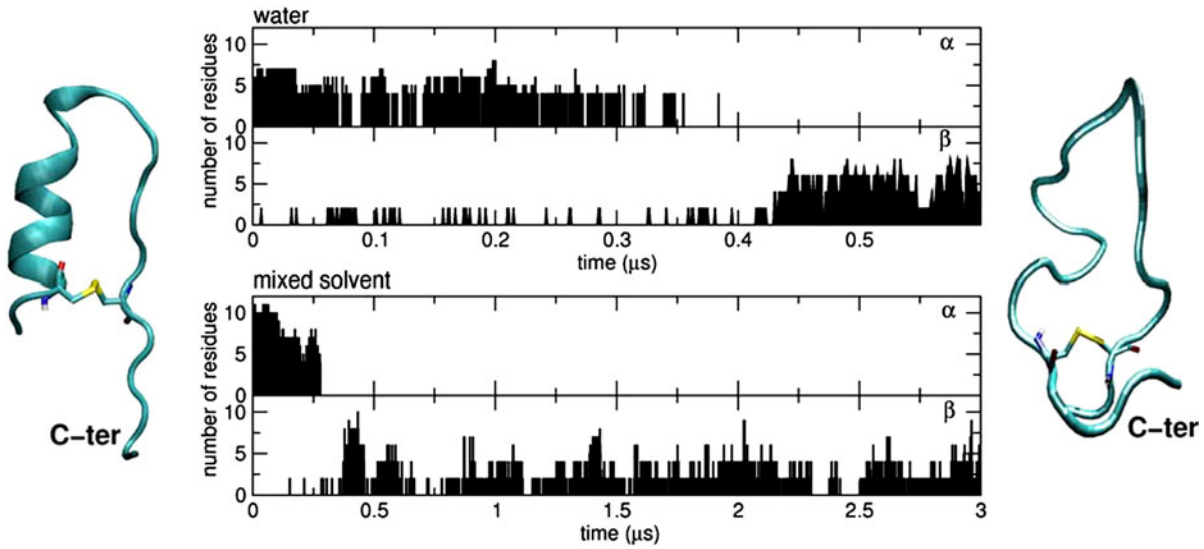

Fig. 2 Time-evolution of the secondary-structure content of LfcinB along the two simulations started from the α-helical conformation in water (*top*) and in membrane-mimicking mixture (*bottom*). The secondary-structure content was calculated with the DSSP program (Kabsch and Sander 1983) and is given as the number of residues adopting the given secondary structure (α-helical or β-sheet). Representative starting (*left*) and final (*right*) configurations are also reported

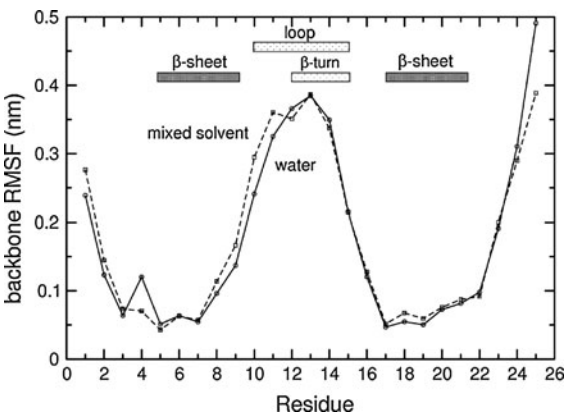

Fig. 3 Root mean square fluctuation (RSMF) of the backbone atoms in the simulations in water (*solid line*) and in mixed solvent (*dashed line*)

mean square deviation (RMSD) plot computed for the best 20 structures in water satisfying the NOE distance restraints (Hwang et al. 1998). On the base of the α_i-NH and sequential NH–NH NOEs found in the NMR spectra (Hwang et al. 1998), a turn has been attributed to the four residues of the loop, K12-L13-G14-A15. The type of turn is here analyzed by evaluating the presence of the $4 \rightarrow 1$ H-bond between the K12CO and A15NH groups, as well as the φ/ψ angles of the (i + 1)th and (i + 2)th residues (L13 and G14, respectively), for the simulation in water. The data are reported in Fig. 4. Three different states are shown to populate the K12-A15 region: (i) a type-II βturn, (ii) a type-I' βturn and (iii) unstructured, with time percentage estimated as 40, 10 and 50%, respectively. Similar results were obtained for the simulation in the mixed solvent.

The lower sensitivity to temperature changes of the NH chemical shifts of Q7, R9, A15, S17 and T19 with respect to other amide protons (Hwang et al. 1998), was ascribed to the engagement of these groups in H-bonds. Our simulation in water reveals that the NH and CO groups of Q7 and R9, belonging to one strand, are respectively engaged with the CO and NH groups of T19 and S17, belonging to the opposite strand, in stable β-sheet H-bonds along the complete run. The NH group of A15 is less permanently engaged in the $4 \rightarrow 1$ H-bond, as evident in the backbone fluctuations reported in Fig. 3. A similar H-bonding network results from the simulation in the mixed solvent.

Strong sequential NH–NH NOEs (Hwang et al. 1998) were observed between R4 and R5 as well as between V21 and R22, indicating the presence of kinks near the disulfide bridge connecting the two

strands. We checked the presence of these kinks in our simulation and, in Fig. 5, we report the Ramachandran plot of the residues R5 and V21, showing φ/ψ values typical of a kinked backbone for the simulation in water. Similar results were obtained in the simulation with the mixed solvent.

The β-hairpin structure, resulting from both the MD simulations and CD spectra performed in aqueous and hydrophobic solutions, presents amphipathic structure. The side-chains of residues F1, C3, W6, W8, M10, I18, C20, F25 form the hydrophobic surface on one side of the sheet, whereas on the opposite side of the sheet, the side-chains of K2, R4, R5, R22, R23 give rise to the hydrophilic surface, as shown on top panel of Fig. 6. Furthermore, while the spatial configuration of the side-chains forming the hydrophilic surface, simulated both in water and in mixed solvent, does not show significant variations with respect to the best 20 structures satisfying the NOE distance restraints in water (Hwang et al. 1998) (data not shown), some differences are observed for the hydrophobic surface.

To further investigate these differences, the radius of gyration (Rg) of the side-chains forming the hydrophobic surface was calculated and reported in the middle panel of Fig. 6. As it can be seen, while the Rg values along the simulation in water are in agreement with those obtained from the best 20 structures satisfying NOE distance restraints in water (Hwang et al. 1998), the Rg values obtained for the simulation in mixed solvent are higher, indicating an enlarged hydrophobic surface. Moreover, we compared the side-chain χ_1 torsion angles of the hydrophobic residues giving rise to this different behavior. The largest differences were found for the two side-chains of W6 and W8. In particular, the distributions of the χ_1 torsion angle of W8 along the simulation in water and in mixed solvent are reported (Fig. 7). While in water the two most populated conformations are characterized by the aromatic ring pointing towards the peptide hydrophobic surface (peaks A and B of Fig. 7), in mixed solvent a high populated conformation, not present in water, is observed with the ring pointing outwards, i.e., towards the solvent (peak C of Fig. 7).

In what follows, the structural organization of the mixed solvent is investigated. Before addressing the local mechanisms through which the mixture stabilizes the peptide conformation, analyses of the global structural properties of the solvent along the simulation were performed showing dynamical partial clustering. Representative snapshots extracted along the 1.1 μs-long β-hairpin simulation (see Fig. 8) clearly show formation of clusters of chloroform and of methanol–water that are very dynamical, i.e., their position, dimension and composition change in time. Previous experimental and computational studies (Moelwyn-Hughes and Missen 1957; Singh et al. 1979; Gratias and Kessler 1998; Mottamal et al. 2007) have shown evidence of analogous

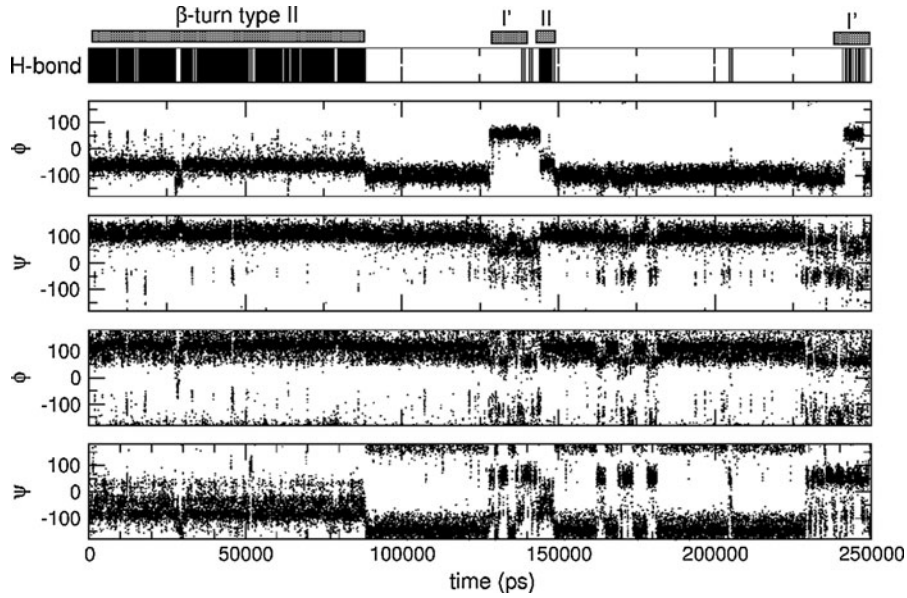

Fig. 4 *Top panel* existence of the turn hydrogen bond between residue ith (K12) and (i + 3)th (A15) along the simulation in water. *Bottom panels* φ/ψ torsion angles of the (i + 1)th residue (L13) and (i + 2)th (G14) along the simulation in water. Similar results are also observed along the 1.1 μs-long simulation in mixed solvent

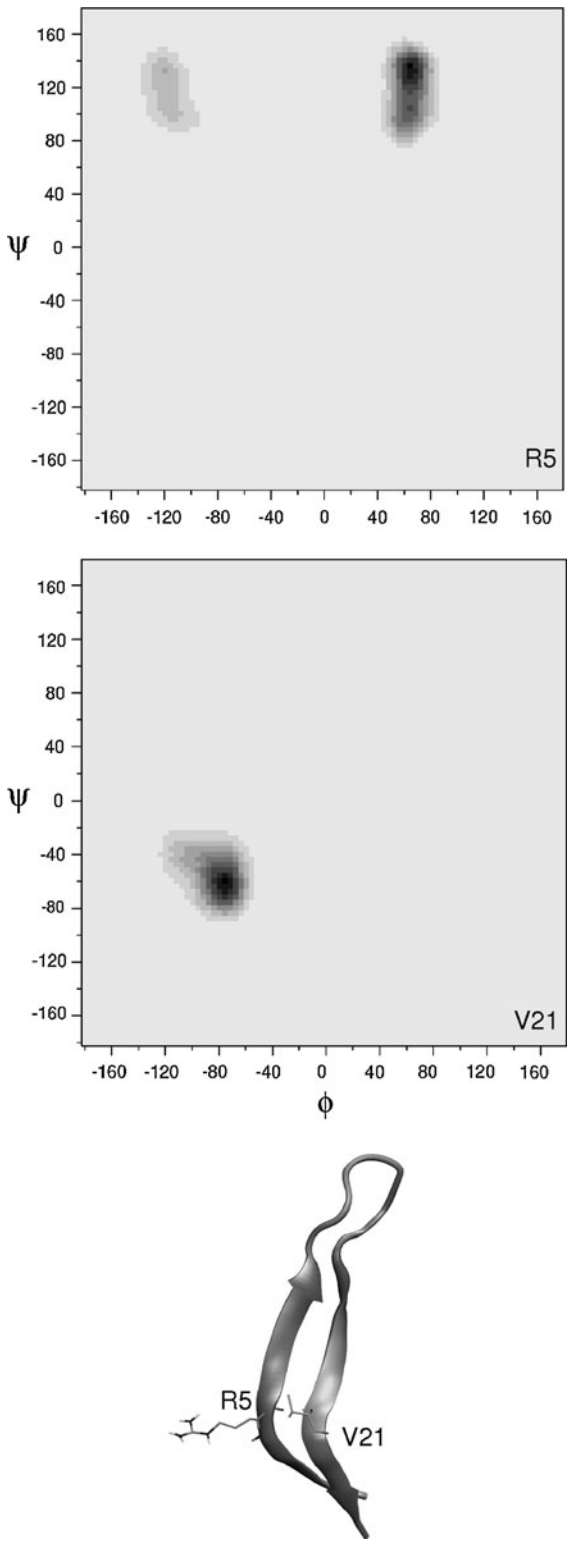

◀ **Fig. 5** Analysis of the kink in the backbone. *Top panel* Ramachandran plot of R5. *Middle panel* Ramachandran plot of V21. *Bottom panel* representative hairpin structure. The results refer to the simulation in water. Similar results are also observed along the 1.1 μs-long simulation in mixed solvent

self-clustering in methanol–chloroform mixtures leading to microscopic heterogeneity. This tendency leads to preferential solvation of the hydrophilic and hydrophobic portions of the peptide by the polar component (methanol and water) and chloroform,

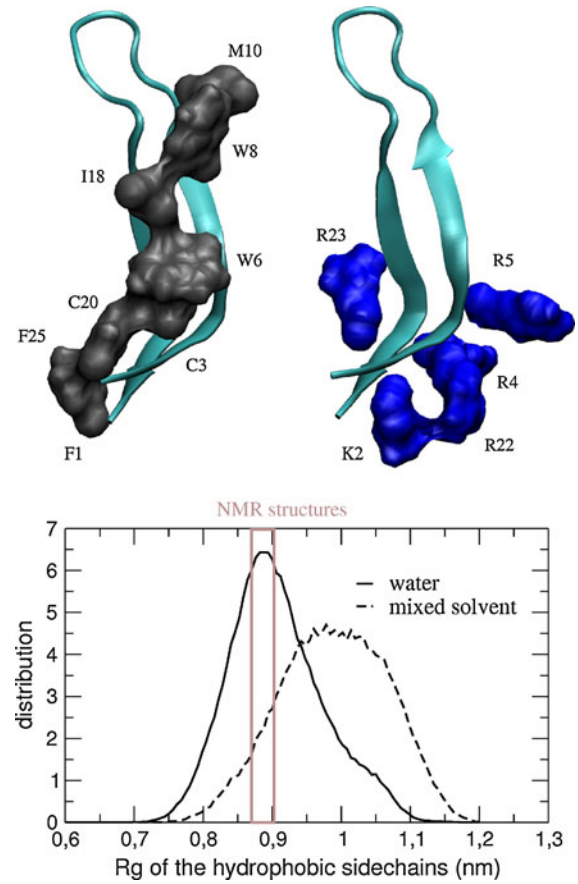

Fig. 6 Analysis of the side-chains. *Top panel* representative structure of the hydrophobic side-chains forming the hydrophobic surface, i.e., residues 1, 3, 6, 8, 10, 18, 20 and 25 (*left*) and of the hydrophilic side-chains that are on the opposite side of the hydrophobic surface, i.e., residues 2, 4, 5, 22 and 23 (*right*) along the simulation in water. *Bottom panel* radius of gyration (*Rg*) of the above mentioned hydrophobic side-chains in water (*solid line*) and in mixed solvent (*dashed line*). The interval highlighted in the *box* indicates the range of radius of gyration of the hydrophobic side-chains in the 20 NMR (Hwang et al. 1998) structures in water

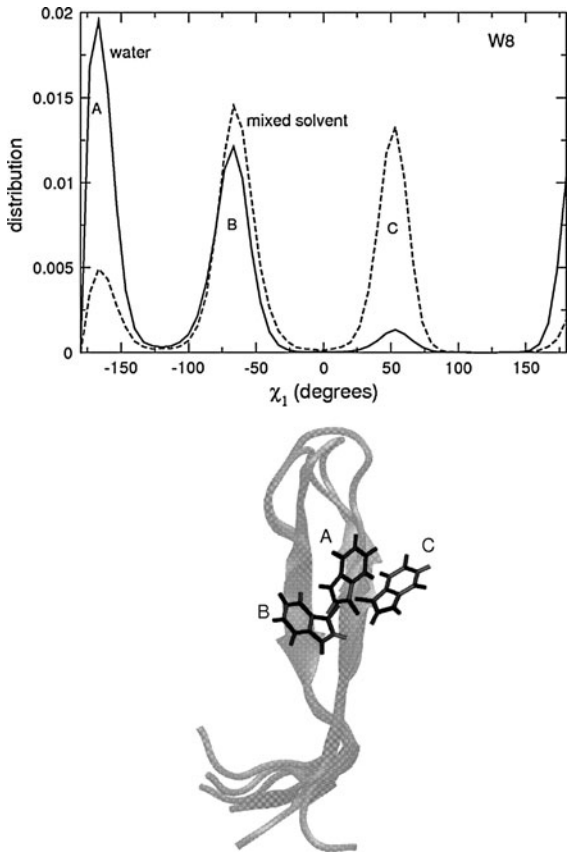

Fig. 7 *Top panel* distribution of the $\chi 1$ torsion angle of the side-chain of W8 in the simulations in water (*solid line*) and in mixed solvent (*dashed line*). *Bottom panel* representative conformations of the side-chain of the three main peaks *A*, *B* and *C*

respectively (see Fig. 9), in agreement with previous work on other molecules (Gratias and Kessler 1998; Mottamal et al. 2007). Hence, the local phase separation of the mixture stabilizing the amphiphilic peptide provides an environment resembling the lipid-water interface of cell membranes. In fact, the water–methanol rich phase surrounding the hydrophilic residues takes on the role of the layer populated by water and charged lipid headgroups, and the chloroform rich phase around the hydrophobic surface takes the function of the apolar tails of the lipid bilayer.

Conclusions

The MD simulations and CD spectra here reported indicate that in membrane-mimicking solutions LfcinB adopts a β-hairpin structure similar to that observed by 2D NMR in water, showing that the amphipathic structure of LfcinB is solvent independent. This amphiphilic β-hairpin conformation favors the clustering of the majority of hydrophobic and hydrophilic residues on opposite sides, likely allowing LfcinB to better interact with the lipopolysaccharides of the bacterial membrane. As a matter of fact, hydrophobic and hydrophilic residues can interact with fatty acyl groups of the lipid bilayer and the phosphodiester groups, respectively, and a more effective partition of interactions can take place upon

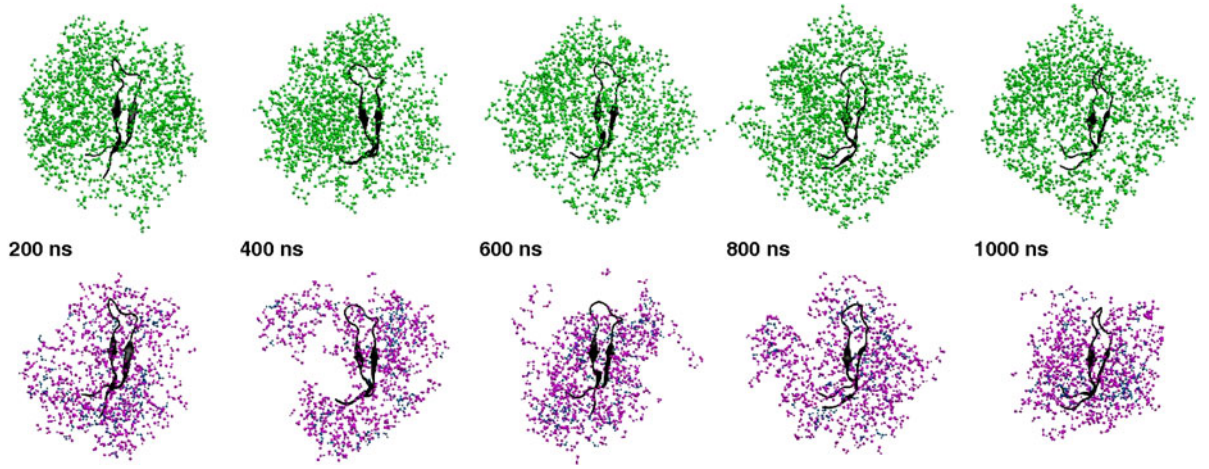

Fig. 8 Snapshots along the 1.1 μs-long MD trajectory of the β-hairpin in mixed solvent showing the variation of the clusters in the mixture. Chloroform and methanol/water molecules are shown in the top and bottom panels, respectively

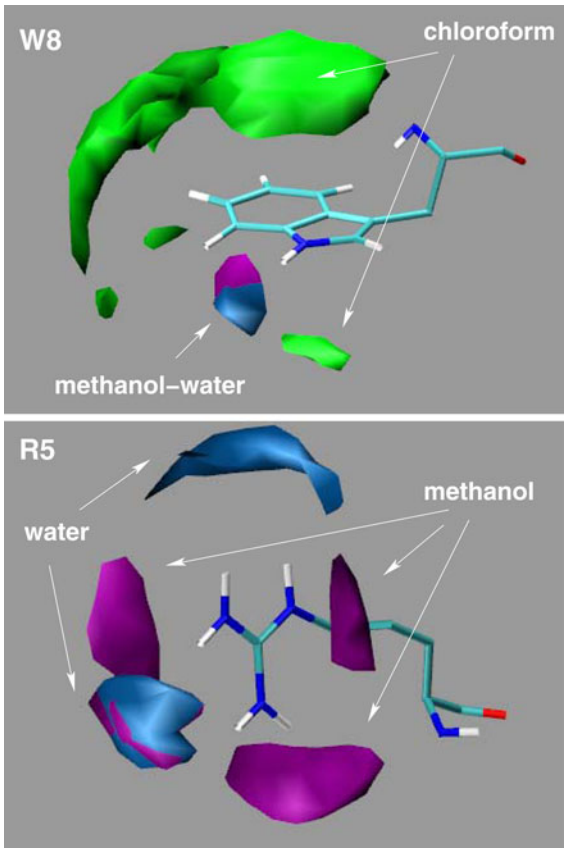

Fig. 9 Spatial distribution function (Kulińska et al. 2000) for chloroform, methanol and water around residue W8 (*top*) and residue R5 (*bottom*) calculated over the 1.1 μs-long MD trajectory of the β-hairpin in mixed solvent. Each curve represents an isosurface in the local coordinate system around the residue in which the local concentration of the corresponding solvent component is 50% of the maximum value of the distribution function. Hydrophilic residues, as R5, are mainly surrounded by methanol and water, while hydrophobic residues, as W8, show a preference for chloroform

binding. This favorable placement of LfcinB side-chains differs from that present in the same fragment of the intact protein LfB, where an α-helix extends from F17 to L29 (F1 to L13 of LfcinB), whereas the segment from S33 to R39 (S17 to R23 of LfcinB) adopts an extended strand in both cases.

These results indicate that the LfcinB β-hairpin structure might play a key role in the interaction with the membrane by spatially segregating hydrophobic from hydrophilic residues. Moreover, the propensity of the W6 and W8 side-chains for a conformational change promoted by an hydrophobic environment, shown in the simulation of LfcinB in mixed solvent, can favor the tryptophans interaction with the interfacial region of the lipid membranes, enhancing the anchoring effect of the indole rings as the peptide penetrates into the hydrocarbon core of the lipid bilayer. This supports the role of the tract RRWQWR as the antimicrobial core of LfcinB.

Acknowledgments This work was supported by the Italian FIRB RBIN04PWNC_001 "Structure, function, dynamics and folding of proteins" founded by MIUR. We also acknowledge the University of Rome "La Sapienza" for financial support with the project "Morfogenesi Molecolare: un approccio multidisciplinare per lo studio del folding e misfolding delle proteine" and CASPUR (Consorzio interuniversitario per le Applicazioni di Supercalcolo Per Universitá e Ricerca) for the use of its computational facilities.

References

Anderson BF, Baker HM, Norris GE, Rice DW, Baker EN (1989) Structure of human lactoferrin: crystallographic structure analysis and refinement at 2.8 Å resolution. J Mol Biol 209:711–734

Anderson JH, Jenssen H, Gutteberg TJ (2003) Lactoferrin and lactoferricin inhibit herpes simplex 1 and 2 infection and exhibit synergy when combined with acyclovir. Antiviral Res 58:209–215

Bals R, Wilson JM (2003) Cathelicidins: a family of multifunctional antimicrobial peptides. Cell Mol Life Sci 60:711–720

Bellamy W, Takase M, Wakabayashi H, Kawase K, Tomita M (1992a) Antibacterial spectrum of lactoferricin B, a potent bactericidal peptide derived from the N-terminal region of bovine lactoferrin. J Appl Bacteriol 73:472–479

Bellamy W, Takase M, Yamauchi K, Wakabayashi H, Kawase K, Tomita M (1992b) Identification of the bactericidal domain of lactoferrin. Biochim Biophys Acta 1121: 130–136

Bellamy W, Yamauchi K, Wakabayashi H, Takase M, Kawase K, Takakura N, Shimamura S, Tomita M (1994) Antifungal properties of lactoferricin B, a peptide derived from the N-terminal region of bovine lactoferrin. Lett Appl Microbiol 18:230–233

Berendsen HJC, Postma JPM, van Gunsteren WF, Di Nola A, Haak JR (1984) Molecular dynamics with coupling to an external bath. J Chem Phys 81:3684–3690

Berendsen HJC, Grigera JR, Straatsma TP (1987) The missing term in effective pair potentials. J Phys Chem 91:6269–6271

Berendsen HJC, van der Spoel D, van Drunen R (1995) Gromacs: a message-passing parallel molecular dynamics implementation. Comp Phys Comm 95:43–56

Boman HG (1995) Peptide antibiotics and their role in innate immunity. Annu Rev Immunol 13:61–92

Brown D, Clarke JHR (1984) A comparison of constant energy, constant temperature, and constant pressure ensembles in molecular dynamics simulations of atomic liquids. Mol Phys 51:1243–1252

Darden T, York D, Pedersen L (1993) Particle mesh Ewald: an N-log(N) method for Ewald sums in large systems. J Chem Phys 98:10089–10092

Eliassen LT, Berge G, Sveinbjørnsson B, Svendsen JS, Vorland LH, Rekdal Ø (2002) Evidence for a direct antitumor mechanism of action of bovine lactoferricin. Anticancer Res 22:2703–2710

Ganz R, Lehrer RI (1999) Antibiotic peptides from higher eukaryotes: biology and applications. Mol Med Today 5: 292–297

Gifford JL, Hunter HN, Vogel HJ (2005) Lactoferricin: a lactoferrin-derived peptide with antimicrobial, antiviral, antitumor and and immunological properties. Cell Mol Life Sci 62:2588–2598

Gratias R, Kessler H (1998) Molecular dynamics study on microheterogeneity and preferential solvatino in methanol/chloroform mixtures. J Phys Chem B 102:2027–2031

Hancock REW (2001) Cationic peptides: effectors in innate immunity and novel antimicrobials. Lancet Infect Dis 1: 156–164

Hunter HN, Demcoe AR, Jenssen H, Gutteberg TJ, Vogel HJ (2005) Human lactoferricin is partially folded in aqueous solution and is better stabilized in a membrane mimetic solvent. Antimicrob Agents Chemother 49:3387–3395

Hwang PM, Zhou N, Shan X, Arrowsmith CH, Vogel HJ (1998) Three-dimensional solution structure of lactoferricin B, an antimicrobial peptide derived from bovine lactoferrin. Biochemistry 37:4288–4298

Kabsch W, Sander C (1983) Dictionary of protein secondary structure: pattern recognition of hydrogen bonded and geometrical features. Biopolymers 22:2577–2637

Kang JH, Lee MK, Kim KL, Haham KS (1996) Structural-biological activity relationships of 11-residue highly basic peptide segment of bovine lactoferrin. Int J Pept Protein Res 48:357–363

Kulińska K, Kuliński T, Lyubartsev A, Laaksonen A, Adamiak RW (2000) Spatial distribution functions as a tool in the analysis of ribonucleic acids hydration—molecular dynamics studies. Comput Chem 24:451–457

Martin E, Gantz T, Lehrer R (1995) Defensins and other endogenous peptide antibiotics of vertebrates. J Leukoc Biol 58:128–136

Moelwyn-Hughes EA, Missen RW (1957) Thermodynamics properties of methyl alcohol-chloromethane solutions. J Phys Chem 61:518–521

Moore SA, Anderson BF, Groom CR, Haridas M, Baker EN (1997) Three-dimensional structure of diferric bovine lactoferrin at 2.8 Å resolution. J Mol Biol 274:222–236

Mottamal M, Shen S, Guembe C, Krilov G (2007) Solvation of transmembrane proteins by isotropic membrane mimetics: a molecular dynamics study. J Phys Chem B 111: 11285–11296

Rekdal Ø, Andersen J, Vorland LH, Svendsen JS (1999) Construction and synthesis of lactoferricin derivatives with enhanced antibacterial activity. J Pept Sci 5:32–45

Roy MK, Kuwabara H, Hara K, Watanabe Y, Tamai Y (2002) Peptides from the N-terminal end of bovine lactoferrin induce apoptosis in human leukemic (HL-60) cells. J Diary Sci 85:2065–2074

Singh PP, Sharma BR, Sidhu KS (1979) Thermodynamics of chloroform and methanol mixtures. Can J Chem 57:387–393

Strøm MB, Rekdal Ø, Svendsen JS (2000) Antibacterial activity of 15 residue lactoferricin derivatives. J Pept Res 56:265–274

Strøm BA, Hang BE, Rekdal Ø, Skar ML, Stensen W, Svendsen JS (2002) Important structural features of 15-residue lactoferricin derivatives and methods for improvement of antimicrobial activity. Biochem Cell Biol 80:65–74

Tomita M, Bellamy W, Takase M, Yamauchi K, Wakabayashi H, Kawase K (1991) Potent antibacterial peptides generated by pepsin digestion of bovine lactoferrin. J Dairy Sci 74:4137–4142

Tomita M, Takase M, Bellamy W, Shimamura S (1994) A review: the active peptide of lactoferrin. Acta Paediatr Jpn 36:585–591

van Gunsteren WF, Billeter SR, Eising AA, Hünenberger PH, Krüger P, Mark AE, Scott WRP, Tironi IG (1996) Biomolecular simulation: the GROMOS96 manual and user guide. Hochschulverlag AG an der ETH Zürich, Zürich

Vivcharuk V, Tomberli B, Tolokh IS, Gray CG (2008) Prediction of binding free energy for adsorption of antimicrobial peptide lactoferricin B on a POPC membrane. Phys Rev E 77:031913

Vogel HJ, Schibli DJ, Jing W, Lohmeier-Vogel EM, Epand RF, Epand RM (2002) Towards a structure-function analysis of bovine lactoferricin and related tryptophan- and arginine-containing peptides. Biochem Cell Biol 80:49–63

Vorland LH, Ulvatne H, Andersen J, Haukland HH, Rekdal Ø, Svendsen JS, Gutteberg TJ (1998) Lactoferricin of bovine origin is more active than lactoferricins of human, murine and caprine origin. Scand J Infect Dis 30:513–517

Waterhouse DV, Johnson WC Jr (1994) Importance of environment in determining secondary structure in proteins. Biochemistry 33:2121–2128

Whitmore L, Wallace BA (2004) DICHROWEB: an online server for protein secondary structure analyses from circular dichroism spectroscopic data. Nucl Acids Res 32:W668–W673

Zasloff M (2002) Antimicrobial peptides of multicellular organisms. Nature 415:389–395

Zhou N, Tieleman DP, Vogel HJ (2004) Molecular dynamics simulations of bovine lactoferricin: turning a helix into a sheet. Biometals 17:217–223